

ANALYSIS OF A DEEP "NON DOUBLE COUPLE" EARTHQUAKE
USING VERY BROADBAND DATA

Keiko Kuge

Earthquake Research Institute, University of Tokyo

Hitoshi Kawakatsu

Geological Survey of Japan

Abstract. We analyze the source mechanism of a deep earthquake beneath Japan on January 1, 1984, whose Harvard centroid moment tensor (CMT) solution significantly deviates from a double couple mechanism. The broadband P-wave ground displacement records show the presence of several distinct phases whose relative amplitudes vary among the stations. We perform very broadband waveform analyses over four different frequency bands: CMT inversion (surface waves (4–5mHz) and long-period body waves (12–20mHz)), waveform inversion using the long-period P, pP and SH waves (~0.04Hz), and broadband P- and pP-wave waveform analysis (0.03–1Hz). We show that the large non double couple solution observed at long periods (>25sec) is very likely to be a manifestation of the presence of subevents with different double couple mechanisms in a single rupture sequence.

Introduction

It is known that radiation patterns of deep earthquakes are usually well explained in terms of double couple (DC) force systems. Some proposed physical mechanisms for deep earthquakes involve non-faulting source mechanisms (for example, a compensated linear-vector dipole (CLVD) [Knopoff and Randall, 1970]). However, seismological evidence favors shear failure as the mechanism for deep earthquakes. Directivity [e.g., Fukao, 1972] and the seismicity analyses [e.g., Billington and Isacks, 1975] suggest that deep earthquakes rupture in the fault planes.

On the other hand, recent systematic studies of deep earthquakes at long periods (>45 seconds) show that some deep earthquakes significantly deviate from DC mechanisms [e.g., Dziewonski and Woodhouse, 1983; Giardini, 1983]. Considering that the isotropic part of a moment tensor is difficult to constrain at long periods, these researchers solved for the deviatoric part of the moment tensor. The deviation of a moment tensor from a DC mechanism is measured by the factor, $\epsilon = -e_2 / \max(|e_1|, |e_3|)$, where e_1 , e_2 , and e_3 are eigenvalues of a moment tensor ($e_1 > e_2 > e_3$) [Giardini, 1983]. Note that $\epsilon = 0$ for a DC mechanism and that $|\epsilon| = 0.5$ for a CLVD. We should resolve the nature of the non-double couple (NDC) deep earthquakes in detail by seismological means and then consider the physical process of deep earthquakes.

It is possible that NDC mechanisms are due to the superposition of several subevents with different DC mechanisms during the rupture process. For example, Sipkin [1986] suggested this as the explanation for a shallow earthquake with a large NDC component. The presence of subevents with different mechanisms has also been observed in the failure process of deep earthquakes [e.g., Strelitz, 1980; Choy and Boatwright, 1981]. It seems reasonable that the NDC mechanisms of deep earthquakes can also best be explained by the presence of subevents with different DC mechanisms.

A deep earthquake occurred beneath Japan on January 1, 1984 (9:03:40.1UT, 33.62°N, 136.80°E, depth=386.0km, $m_b=6.4$, ISC). Ekström et al. [1986] pointed out that the centroid moment tensor (CMT) solution significantly deviates from a DC mechanism. Their single station CMT analysis [Ekström et al., 1986] also showed that the large NDC component cannot be an artifact introduced by unmodelled propagation effects.

In the present paper, we examine the deviatoric part of the moment tensor and investigate the possibility that the large NDC solution observed at long periods is caused by the presence of several subevents with different DC mechanisms in the single rupture sequence. To obtain a coherent solution for the rupture process, we perform a very broadband waveform analysis and model various phases of seismograms in a very broad frequency band (4mHz~1Hz). Such a very broadband analysis was first performed by Ekström [1987] for shallow earthquakes.

Very Broadband Waveform Analysis

We model seismograms over four different frequency bands (Figure 1); the CMT inversion for the surface waves

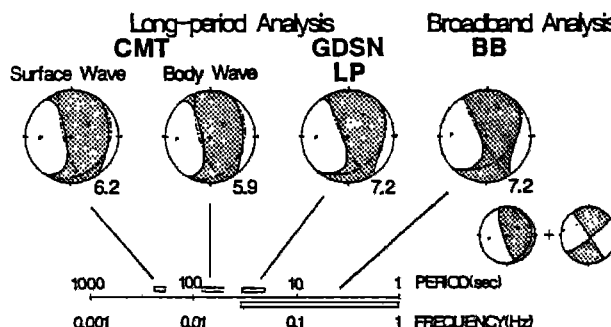


Fig. 1. Comparisons of the moment tensor solutions obtained from the four different frequency bands.

and the long-period body waves, the waveform inversion for GDSN long-period P, pP and SH waves, and the broadband P- and pP-wave waveform analysis. Note that we estimate focal mechanism solutions for each waveform inversion independently. Table 1 and Figure 1 summarize the results.

Table 1. Source mechanism solutions

| | CMT surface | CMT body | GDSN LP | BB |
|------------|------------------|------------------|------------------|------------------|
| M_0 | 6.20 | 5.91 | 7.23 | 7.18 |
| M_{xx} | 2.64 ± 0.13 | 2.31 ± 0.11 | 3.09 ± 0.14 | 4.15 ± 0.14 |
| M_{yy} | -5.37 ± 0.19 | -4.06 ± 0.16 | -5.06 ± 0.13 | -6.06 ± 0.14 |
| M_{zz} | 2.73 ± 0.09 | 1.76 ± 0.08 | 1.97 ± 0.08 | 1.91 ± 0.04 |
| M_{xy} | -0.46 ± 0.14 | 0.02 ± 0.09 | 0.59 ± 0.12 | 1.11 ± 0.14 |
| M_{xz} | 1.09 ± 0.04 | 1.06 ± 0.07 | 2.20 ± 0.06 | 1.92 ± 0.04 |
| M_{yz} | 4.45 ± 0.09 | 4.93 ± 0.11 | 5.43 ± 0.11 | 4.51 ± 0.06 |
| ϵ | -0.33 | -0.29 | -0.20 | -0.23 |

Unit of M_0 and M_{ij} is $\times 10^{26}$ dyne-cm.

Long-period Analysis

CMT inversion. Although the CMT solutions have been reported by Ekström et al. [1986], we reanalyze surface waves and long-period body waves using a CMT inversion program written locally. The surface waves are band-pass filtered between 4.0 and 5.0mHz. Only the minor arc wave trains are modeled. For the long-period body waves, we use the wave trains from the P arrivals to just before the Love wave arrivals. They are band-pass filtered between 12 and 20mHz and most of the energy is from S and multiple S waves. We used 80 records for surface waves and 77 records for body waves at 20 GDSN, 11 IDA and 3 GEOSCOPE stations. The solutions are consistent with the solution of Ekström et al. [1986]. As Ekström et al. [1986] pointed out, this similarity can be seen even in the single-station CMT solutions, which we have also confirmed from the surface wave inversion.

GDSN long-period P, pP and SH waves. Using a moment tensor inversion method based on a ray theory, we model the P, pP and SH waveforms of GDSN long-period channel whose peak frequencies are around 40mHz, which can be considered as an independent dataset from that used in the CMT inversion. Data are from ANMO (only pP wave), CTAO, KONO, COL, HON, JAS, KEV, LON (only P, pP wave), RSNT, RSON, and RSSD. Although we assume water layers at reflection points of pP waves to CTAO and HON, they are not crucial to our result because of GDSN long-period responses. The parameterization scheme for the inversion closely follows Nábělek [1984]. We estimate only the source time function and the moment tensor. The source time function is parameterized by overlapping isosceles triangles whose half duration is 2 sec. Each seismogram is weighted by the inverse of its power.

NDC components at long periods. The solutions in three different frequency bands at long periods are consistent with each other. Large and similar NDC components ($\epsilon = -0.3 \sim -0.2$) can be seen in all of the solutions. This rules out the possibility that the NDC component is caused by local structure along station-source

paths, because different phases go along different paths. It is also difficult to consider that random errors simultaneously produce all of the large NDC solutions. From the analysis of long-period data, we thus conclude that there exists a large NDC component in the deviatoric part of the moment tensor.

Broadband Analysis

Next, we consider the large NDC mechanism by analyzing P and pP waveforms from the broadband ground displacement seismograms. The data are deconvolved from GDSN long-period and short-period records following Harvey and Choy [1982], or from GDSN intermediate-period records. The pass-band of the filter is between 0.03 and 1.0Hz. Most of the available GDSN stations are located in North America and Europe. In order to supplement the station coverage, we also use pP waveforms at GDSN stations whose reflection points are beneath land, and P waveforms from WWSSN long-period displacement records. WWSSN stations to the west (i.e., NDI, POO, and SNG) are, however, excluded because the large amplitude records impeded hand-digitizing the details of the waveforms. Data are from COL, LON, RSNT, RSON, RSSD, HON (only P), CTAO (only P), KEV and KONO (only P) of the GDSN stations and the GRF array, and IST, MUN, TAU, RIV and RAB of the WWSSN stations. Some waveforms are shown in Figure 2. Two major peaks

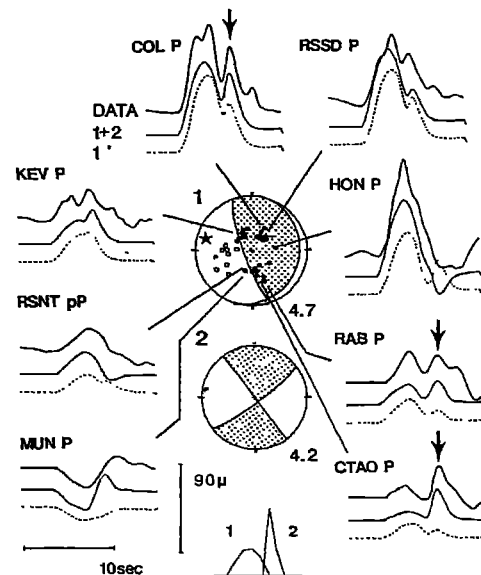


Fig. 2. Solutions derived from broadband analysis. Two DC mechanisms on lower hemispheres, source time functions, and P- and pP-wave displacement seismograms. Initial motions in WWSSN and GDSN long-period records are plotted on the solution for the first subevent. A star symbol represents the relative location of the second subevent on the upper hemisphere to the initial rupture. Upper and middle waveforms represent the observations and the synthetics computed from two different focal mechanisms. Lower waveforms are the synthetics under an assumption of two subevents with the same focal mechanism. The different mechanism is essential for large amplitudes of the second subevents at stations to the south and the north (see arrows).

are observed in P-wave seismograms at stations to the south and the north; e.g., COL, CTAO, and RAB. The second phases arrive around 5 seconds after the onset of the initial phase. PcP phases are expected to arrive much later for these stations; thus the second phases must be intrinsic to the source. The relative amplitudes of the two phases change from one station to another (CTAO and COL). We thus postulate two subevents with different DC mechanisms.

Because we allow subevents to have different focal mechanisms, the parameters to be estimated are origin times, locations, source time functions, and focal mechanisms of all subevents. It is not possible to simultaneously estimate such many parameters in a single inversion. So our analysis takes several steps. By measuring the differential times of various two phases, we first identify the second subevent in each seismogram by trial and error and determine the relative time and location of the second event in the directivity analysis (Figure 3).

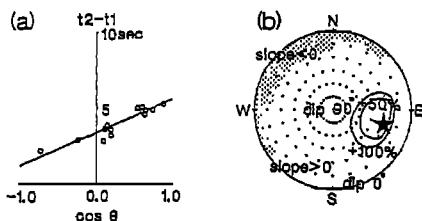


Fig. 3. Directivity analysis for the second subevent. (a) Directivity of the differential times of two phases when the residual becomes minimum. θ is the angle between the station direction and the direction indicated by a star symbol in (b). The slope and y-intercept of the best-fit line give the distance and delay time of the second subevent. (b) Crosses indicate all the dip and azimuth angles for which we examined directivities. Contours represent increase of the squared residuals relative to the minimum value obtained at the star position. A dotted area corresponds to the negative slope of the best-fit line.

Next we obtain the preliminary focal mechanisms by an iterative inversion for the identified subevents. We first determine only the mechanism of the first event. The mechanism of the second subevent is, then, estimated to model the observed waveforms from which the synthetic waveforms of the first subevent have been subtracted. Finally, we perform a simultaneous waveform inversion for the source mechanisms and the source time functions of all considered subevents, using the solution of the previous iterative approach as the initial values. The inversion method is based on Nábělek [1984]. Note that the locations of the subevents are fixed during the analysis once they are determined from the directivity analysis.

Figure 2 and Table 2 show the results. The source mechanism of each subevent is constrained to be a DC mechanism. The half widths of the triangle elements for the source time functions are 1.0 sec for the first subevent to get a stable solution and 0.8 sec for the second one to model the observed arrival-to-peak time at the GDSN stations (1.1 ± 0.3 sec).

The second subevent is estimated to be located 20 km almost west of the initial rupture, near the shallow dipping

Table 2. DC solutions for two subevents

| | strike ($^{\circ}$) | dip ($^{\circ}$) | slip ($^{\circ}$) | M_0 (10^{26} dyne-cm) |
|---|--------------------------|-----------------------|------------------------|-------------------------------|
| 1 | 160.4 ± 0.6 | 77.9 ± 0.3 | 81.5 ± 1.5 | 4.74 ± 0.09 |
| 2 | 323.4 ± 0.6 | 89.5 ± 0.5 | 171.2 ± 0.5 | 4.15 ± 0.20 |

plane of the first subevent which is likely to be the fault plane, and to occur 3.4 sec after the initial rupture. Sugi et al. [1989] and Sagiya [1989] investigated spatio-temporal moment release on the shallow dipping planes. They, however, assumed a single DC source mechanism.

The estimated mechanism of the first subevent is a dominant down-dip compression type. It is consistent with initial motions in WWSSN and GDSN long-period records. On the other hand, the mechanism of the second subevent is almost a pure left-lateral strike slip type. The scalar moments is almost the same. Figure 2 compares the synthetic and observed waveforms. Middle solid lines correspond to the synthetic waveforms computed from the two DC mechanisms shown in this figure. For comparison, we also show the synthetic waveforms (dotted lines) resulted from a single moment tensor inversion when we assume that the two subevents have the same mechanisms. In the case of the single mechanism inversion, synthetic waveforms apparently fail to model large amplitudes of the second phases to southern and northern stations (e.g., CTAO, RAB and COL). Varying the focal mechanisms of the two subevents is thus essential to model the observed waveforms at those stations. The two DC mechanisms reduce 41% of the total squared residuals resulted from the single mechanism.

The moment tensor solution from the broadband analysis, obtained by summing the two DC subevents, is shown in Figure 1 and Table 1 under the label BB. This solution, including a large NDC component, is very similar to those obtained from the long period analyses. We suggest that the presence of the two subevents with different DC mechanisms is the cause of the large NDC component observed in the long period analyses.

Discussion

In the broadband analysis of the previous section, we constrained each subevent to have a DC mechanism. In Figure 4 we show the solution of the moment tensor inversion, in which the subevents are solved for moment tensors, instead of DC mechanisms. In this inversion we impose the additional constraint that the sum of the moment tensors should be equal to the CMT solution (body waves). Introducing this constraint in the inversion is supported by our consistent solutions from the very

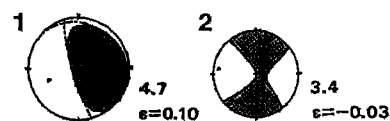


Fig. 4. Moment tensor solutions of the two subevents (see Discussion).

broadband waveform analyses. The estimated moment tensors of the both subevents have small NDC components and are close to the two DC mechanisms obtained in the previous section. We, therefore, consider that our result in the broadband waveform analysis is reliable.

Although we inverted for only two subevents in the present paper, a few more subevents are likely to exist in the rupture process of the first subevent. We can see peaks at the northeastern stations (e.g., COL) in Figure 2 which we failed to model. We can not rule out the possibility of the change of the source mechanisms within the first subevent. Although we do not attempt to model the detail of the first subevent here, we simply point out that the change of the DC mechanism does not always result in the presence of NDC components which may be observed at long periods. For example, the moment tensor obtained by summing two DC mechanisms which share the same N-axis does not have any NDC component.

The two subevents determined by the broadband analysis have significant differences both in the mechanisms and in the source time functions (Figure 2). The mechanism of the first event is the dominant one of the deep earthquakes in the Izu-Bonin area. We, however, note that in the published Harvard CMT solutions [e.g., Dziewonski and Woodhouse, 1983], there exist a few deep earthquakes in the area which have large strike slip components as does the second subevent. Although the scalar moments of the two subevents are almost the same, the duration of the moment release is much longer for the first subevent. This may be a suggestion of differences in the dynamic rupture process, not only the focal mechanism.

Summary

We have obtained consistent source mechanism solutions in a very broad frequency band by analyzing the wave trains of various phases. Two subevents with different double couple focal mechanisms are obtained in the broadband analysis; the combination of the two double couple mechanisms reproduces the moment tensor solutions with large non double couple components obtained from the long-period analyses. This suggests that the non double couple component observed at the long periods is due to the complexity of the rupture process and that the presence of this deep "non double couple" earthquake does not require any new exotic non-double-couple physical mechanisms for deep earthquakes.

We believe that very broadband studies of the rupture process are important for understanding the nature of the non double couple components of earthquakes, as well as the physical mechanism of deep earthquakes.

Acknowledgments. We are grateful to N. Sugi for allowing us to use her digitized WWSSN records, to M. Kikuchi for sending them, and to R. Kind for sending the data at the GRF array. R. J. Geller, K. Shimazaki and M. Takeo critically reviewed the manuscript.

References

- Billington, S., and Isacks, B. L., Identification of fault planes associated with deep earthquakes, *Geophys. Res. Lett.*, **2**, 63-66, 1975.
- Choy, G. L., and Boatwright, J., The rupture characteristics of two deep earthquakes inferred from broadband GDSN data, *Bull. Seism. Soc. Amer.*, **71**, 691-711, 1981.
- Dziewonski, A. M., and Woodhouse, J. H., Studies of the seismic source using normal-mode theory, in *Earthquakes: observation, theory and interpretation*, Kanamori, H. ed., pp. 45-137, 1983.
- Ekström, G., A broad band method of earthquake analysis, Ph. D. thesis, Harvard Univ., 216 pp., Cambridge, Massachusetts, April 1987.
- Ekström, G., Dziewonski, A. M., and Stein, J. M., Single station CMT; application to the Michoacan, Mexico, earthquake of September 19, 1985, *Geophys. Res. Lett.*, **13**, 173-176, 1986.
- Fukao, Y., Source process of a large deep-focus earthquake and its tectonic implications—the western Brazil earthquake of 1963, *Phys. Earth Planet. Inter.*, **5**, 61-76, 1972.
- Giardini, D., Regional deviation of earthquake source mechanisms from the <<double-couple>> model, in *Earthquakes: observation, theory and interpretation*, Kanamori, H. ed. pp. 345-353, 1983.
- Harvey, D., and Choy, G. L., Broad-band deconvolution of GDSN data, *Geophys. J. R. astr. Soc.*, **69**, 659-668, 1982.
- Knopoff, L., and Randall M. J., The compensated linear-vector dipole: a possible mechanism for deep earthquakes, *J. Geophys. Res.*, **75**, 4957-4963, 1970.
- Nábělek, J. L., Determination of earthquake source parameters from inversion of body waves, Ph. D. thesis, 361 pp., Mass. Inst. of Technol., Cambridge, Massachusetts, January 1984.
- Sagiya, T., Imaging of earthquake source processes from waveform inversions using ABIC, Master thesis, Univ. of Tokyo, Tokyo (in Japanese), 1989.
- Sipkin, S. A., Interpretation of non-double-couple earthquake mechanisms derived from moment tensor inversion, *J. Geophys. Res.*, **91**, 531-547, 1986.
- Strelitz, R. A., The fate of the downgoing slab: a study of the moment tensors from body waves of complex deep-focus earthquakes, *Phys. Earth Planet. Inter.*, **21**, 83-96, 1980.
- Sugi, N., Kikuchi, M., and Fukao, Y., Mode of stress release within a subducting slab of lithosphere: implication of source mechanism of deep and intermediate- depth earthquakes, *Phys. Earth Planet. Inter.*, **55**, 106-125, 1989.

K. Kuge, Earthquake Research Institute, University of Tokyo, Tokyo 113 Japan.

H. Kawakatsu, Geological Survey of Japan, Tsukuba 305 Japan.

(Received: December 29, 1989)

Accepted: January 11, 1990)